

## Aniline monomer VMI and further calculation results

Electronic Supplementary Information (ESI) for article

### Photodissociation of aniline N–H bond in clusters of different nature

Viktoriya Poterya,<sup>a</sup> Dana Nachtigallová,<sup>\*b</sup> Jozef Lengyel,<sup>a</sup> and Michal Fárnik<sup>\*a</sup>

<sup>a</sup> J. Heyrovský Institute of Physical Chemistry v.v.i., Czech Academy of Sciences, Dolejškova 3, 18223 Prague, Czech Republic. Fax: +4202 8658 2307; Tel: +4202 6605 3206; E-mail: [michal.farnik@jh-inst.cas.cz](mailto:michal.farnik@jh-inst.cas.cz)

<sup>b</sup> Institute of Organic Chemistry and Biochemistry v.v.i., Czech Academy of Sciences, Flemingovo nám. 2, 16610 Prague 6, Czech Republic. ; E-mail: [dana.nachtigalova@marge.uochb.cas.cz](mailto:dana.nachtigalova@marge.uochb.cas.cz)

#### Experiment: Photodissociation of an isolated aniline molecule

At low He pressure of 0.8 bar and aniline reservoir at the room temperature we assume that only monomers are present in the molecular beam. This assumption is supported by the mass spectra exhibiting only the mass peaks corresponding to the ionization of an isolated aniline molecule. An example VMI of H-atoms originating from isolated aniline molecules photodissociated at 243 nm (5.1 eV) is shown in the inset in **Fig. S1**.

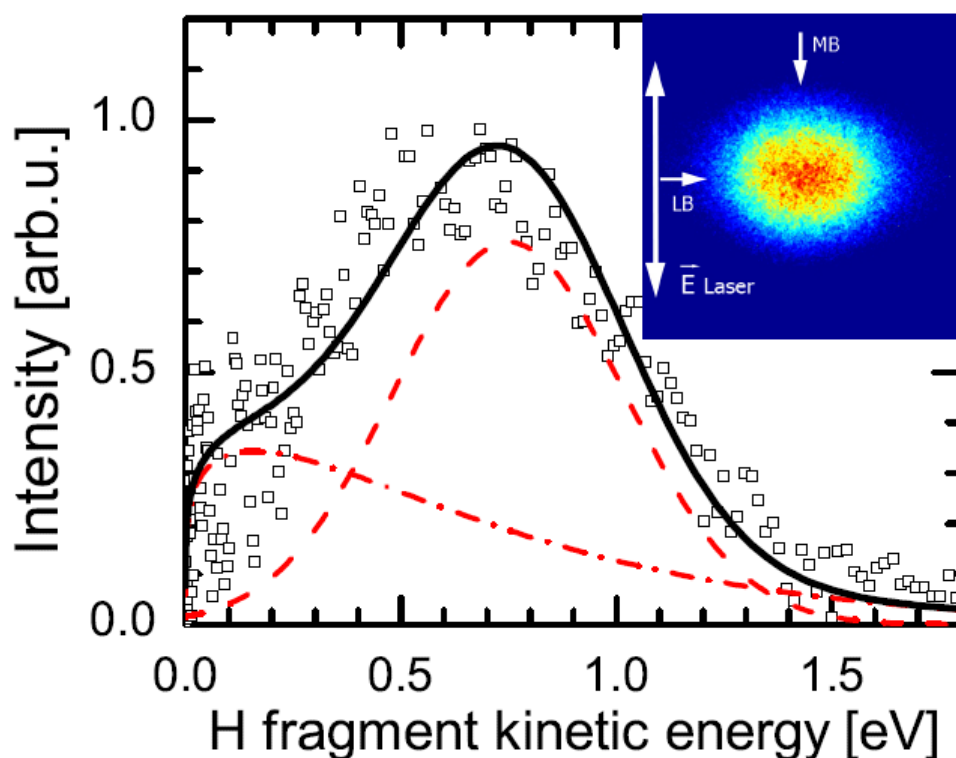


**Fig. S1:** (a) The H fragment KED from the 243 nm photodissociation of aniline molecule. The KED is decomposed to the contribution of the fast (A) and slow (B) fragments dashed and dash-dotted lines, respectively, the solid line represents their sum fitting the experimental points. The inset shows the raw velocity map image, arrows indicate laser and molecular beam direction and the polarization of the laser beam.

The present KED is in good agreement with similar spectra observed previously at comparable dissociation energies.<sup>1,2</sup> It was decoupled into the two components shown by the red lines in **Fig. S1**: (A) a Gaussian peak centered approximately around 0.8 eV. This peak was previously and assigned to a fast N-H bond fission along the  $\pi\sigma^*$  surface.<sup>1,2</sup> (B) a statistical distribution peaking at very low energies around 0.2 eV with a tail extending towards 1.5 eV assigned to the decay of excited  $S_0$  state populated through the  $1^1\pi\sigma^*/S_0$  conical intersection.<sup>1,2</sup>

It ought to be mentioned that attention has to be paid to multiphoton processes. The observed images, like the one in **Fig. S1**, agree with the images obtained in the time resolved experiments of Roberts et al.<sup>1</sup> However, in these pump-probe experiments,<sup>1</sup> a negative time delay (243 nm probe before the pump pulse) was used to determine the contribution of multiphoton processes caused by the 243 nm probe. The signal due to these multiphoton processes was then subtracted from KEDs. In our one-color 243 nm experiments these multiphoton processes are unavoidable. This wavelength is used for molecule photodissociation as well as for H-fragment (2+1) REMPI ionization, i.e. in total 4 photons are required for the process. Lowering the photon flux thus decreases the overall signal and it is difficult to obtain images without any contribution of multiphoton processes. Besides, some  $H^+$  signal can originate from multiphoton induced dissociative ionization.<sup>1,2</sup> Therefore, we have carefully investigated the photon flux dependence within our experimentally accessible range  $10^{27}$ - $10^{28}$  photons $\cdot$ cm $^{-2}$ s $^{-1}$  and determined a multiphoton contribution to our KED spectra which was subtracted from the KEDs. Since this analysis provided the spectrum in **Fig. S1** consistent with the previous investigations of isolated aniline molecules<sup>1,2</sup> we implemented it also to subtract the multiphoton processes from the cluster KEDs.

We have determined the resonance wavelengths by scanning the dye laser across the resonance and observing the total H-fragment signal on the scope. The off-resonance signal was less than 10% of the resonance signal. This also suggests that the  $H^+$  contribution from multiphoton ionization and subsequent ion fragmentation is not overwhelming.

## Theoretical Results

### Isolated aniline

The results of vertical excitation energies of the three lowest excited states calculated at the TD-LC- $\omega$ PBE are compared with previously reported computational and experimental results

in **Table S1**. In agreement with those results the first three excited states are ordered with respect to their energies as  $1^1\pi\pi^*$ ,  $1^1\pi\sigma^*$  and  $2^1\pi\pi^*$  states. In agreement with previously reported results the  $1^1\pi\sigma^*$  state is of Rydberg character localized on the  $\text{NH}_2$  group.

**Table S1:** Calculated Vertical Excitation Energies (eV) and oscillator strengths (f) for aniline

State	TD-LC- $\omega$ PBE (f)	TD-CAM-B3LYP <sup>1</sup>	EOM-CCSD(T) <sup>2,3</sup>
$1^1\pi\pi^*$	5.037 (0.036)	4.88	4.71
$1^1\pi\text{Ryd}_{\text{NH}_2}$	5.581 (0.027)	4.96	4.90
$2^1\pi\pi^*$	5.772 (0.115)	5.53	5.75

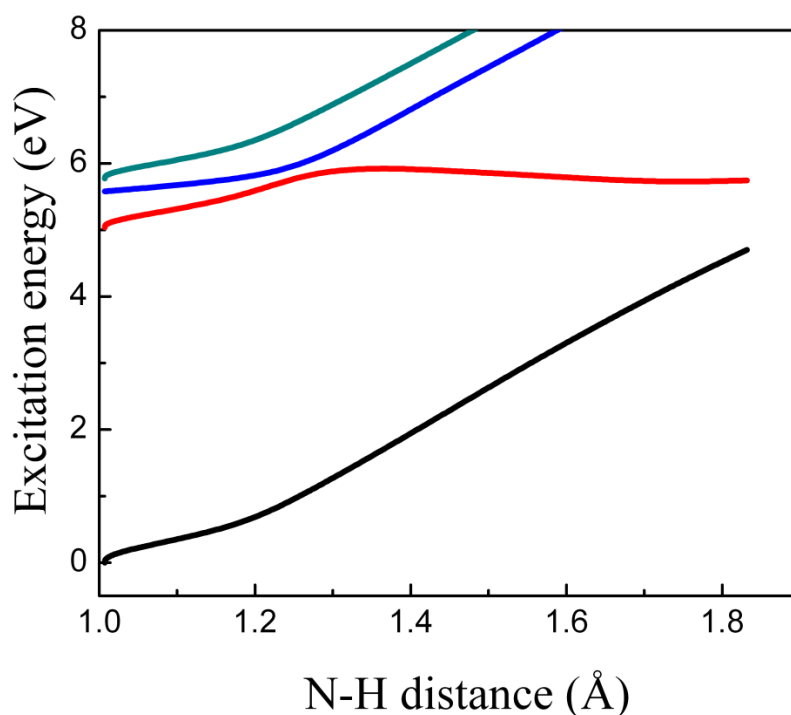


**Fig. S2:** Linear interpolation curve between the Franck-Condon region and  $1^1\pi\sigma^*/S_0$  calculated for the isolated  $\text{PhNH}_2$ . In the vFC region the red, blue and green curves correspond to states of  $1^1\pi\pi^*$ ,  $1^1\pi\text{Ryd}_{\text{NH}_2}$  and  $2^1\pi\pi^*$  characters, respectively.

### Aniline dimers

The results of calculations of the vertical excitation energies are given in **Table S3**. In case of  $(\text{PhNH}_2)_2$ -I the excited states are delocalized between the two monomers as a result of their symmetrical arrangement. With respect to the monomer a small stabilization of 0.05 – 0.18 eV is observed for the first two excited states of  $\pi\pi^*$  character. This finding is in agreement

with the experimentally observed changes of the absorption spectra due to the dimerization.<sup>5</sup> The third and fourth excited states of  $\pi\pi^*$  character are destabilized by a negligible amount (less than 0.05 eV) with respect to  $2^1\pi\pi^*$  states of the monomer. The Rydberg states are destabilized by 0.42 and 0.46 eV, respectively, which causes a change of ordering of the states. Similar results were observed also in the absorption spectra of  $(\text{PhNH}_2)_2\text{-II}$ .

**Table S2.** Vertical excitation energies (in eV) of  $(\text{PhNH}_2)_2$  clusters

$(\text{PhNH}_2)_2\text{-I}$		$(\text{PhNH}_2)_2\text{-II}$	
State		State	
$1^1\pi\pi^*$	4.876 (0.000)	$1^1\pi\pi^*(\text{deloc})$	4.918 (0.040)
$2^1\pi\pi^*$	4.987 (0.059)	$2^1\pi\pi^*(\text{loc})$	5.114 (0.027)
$3^1\pi\pi^*$	5.597 (0.000)	$3^1\pi\pi^*(\text{loc})$	5.592 (0.223)
$4^1\pi\pi^*$	5.629 (0.217)	$1^1\pi\text{Ryd}_{\text{NH}_2}$	5.615 (0.002)
$1^1\pi\text{Ryd}_{\text{NH}_2}$	5.997 (0.014)	$4^1\pi\pi^*(\text{deloc})$	5.776 (0.092)
$2^1\pi\text{Ryd}_{\text{NH}_2}$	6.043 (0.000)	$2^1\pi\text{Ryd}_{\text{NH}_2}$	6.019 (0.030)

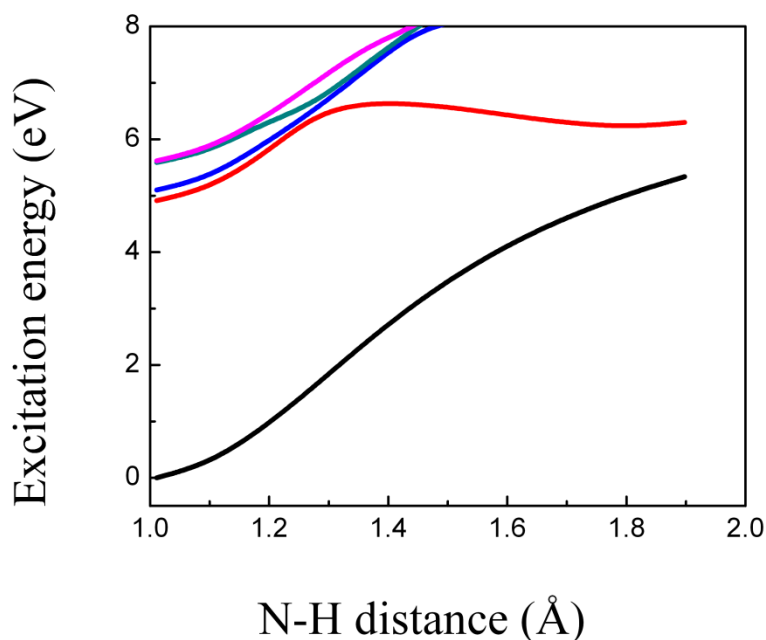


**Fig. S3:** Linear interpolation curve between the Franck-Condon region and  $1^1\pi\sigma^*/S_0$  calculated for  $(\text{PhNH}_2)_2\text{-II}$  dimer. The ordering of the states in the vFC region is shown in **Table S2**.

### Aniline trimers

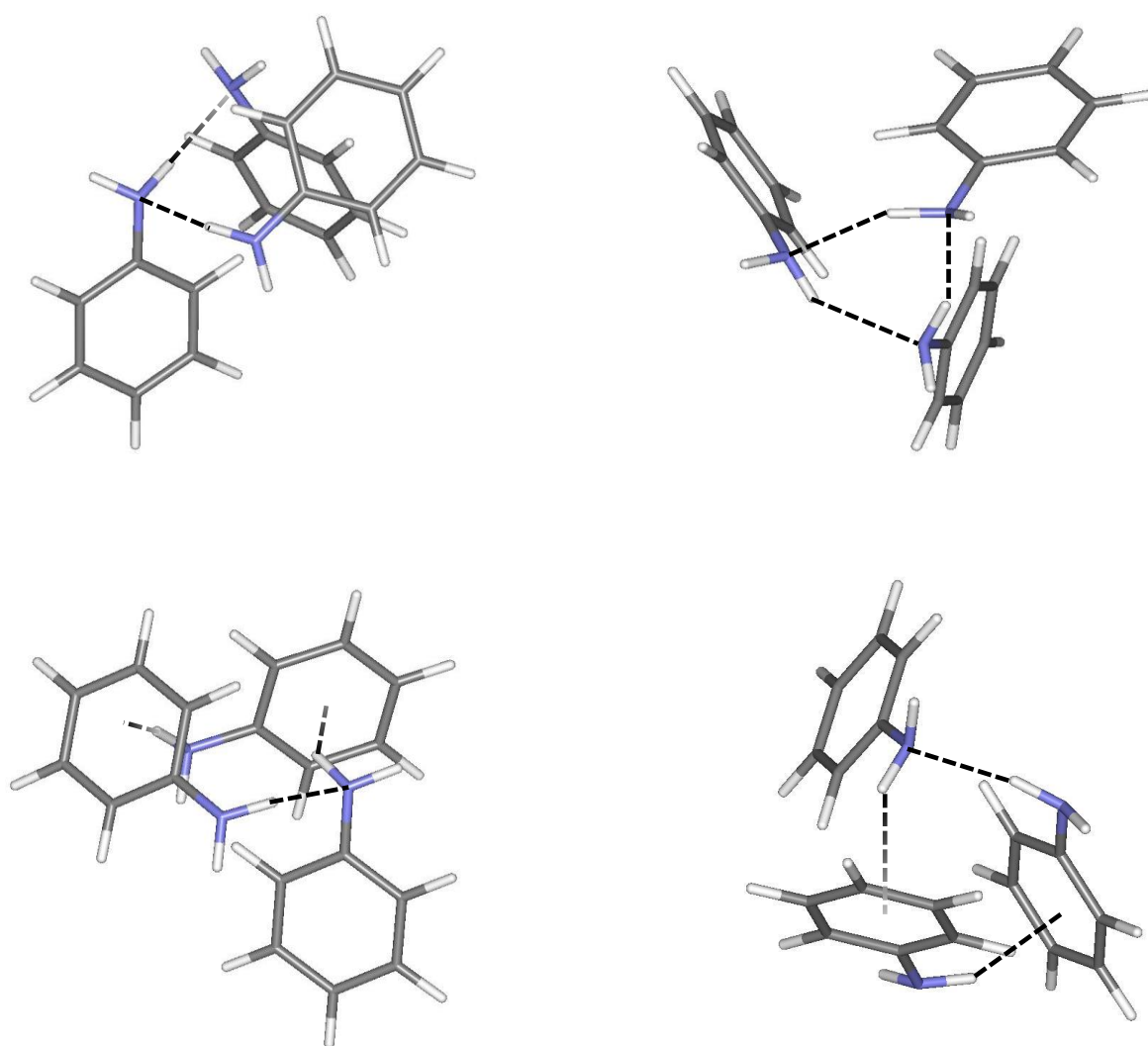


**Fig. S4:** The structures of the four lowest  $\text{PhNH}_2$  trimers with the relative energies within 1 kcal/mol.

### Aniline-water clusters

The results of the vertical excitation energies together with the oscillator strengths of  $\text{PhNH}_2 \cdot (\text{H}_2\text{O})_2$  are given in **Table S3**. The presence of water molecules causes a red shift of the vertical excitation energies of both  $\pi\pi^*$  valence states by 0.2 – 0.3 eV. This result agrees with a general observation of stabilizing of states of  $\pi\pi^*$  due to the presence of polar solvent.

Contrary to that the Rydberg states localized on the NH<sub>2</sub> group are pushed to higher energies above the valence  $\pi\pi^*$  states. In fact, we did not identify any Rydberg state with such character in the energy region which corresponding to experimental condition. Instead the states with Rydberg character localized on the clustering water molecules appear in the energetic region corresponding to valence states.

**Table S3:** Vertical excitation energies (in eV) of PhNH<sub>2</sub>.(H<sub>2</sub>O)<sub>2</sub> clusters

PhNH <sub>2</sub> .(H <sub>2</sub> O) <sub>2</sub> -I		PhNH <sub>2</sub> .(H <sub>2</sub> O) <sub>2</sub> -II	
State		State	
1 <sup>1</sup> $\pi\pi^*$	4.853 (0.048)	1 <sup>1</sup> $\pi\pi^*$	4.808 (0.048)
2 <sup>1</sup> $\pi\pi^*$	5.570 (0.159)	1 $\pi$ Ryd <sub>H2O</sub>	5.300 (0.002)
1 $\pi$ Ryd <sub>H2O</sub>	5.680 (0.012)	2 <sup>1</sup> $\pi\pi^*$	5.469 (0.168)
		1 $\pi$ Ryd <sub>H2O</sub>	5.657 (0.001)

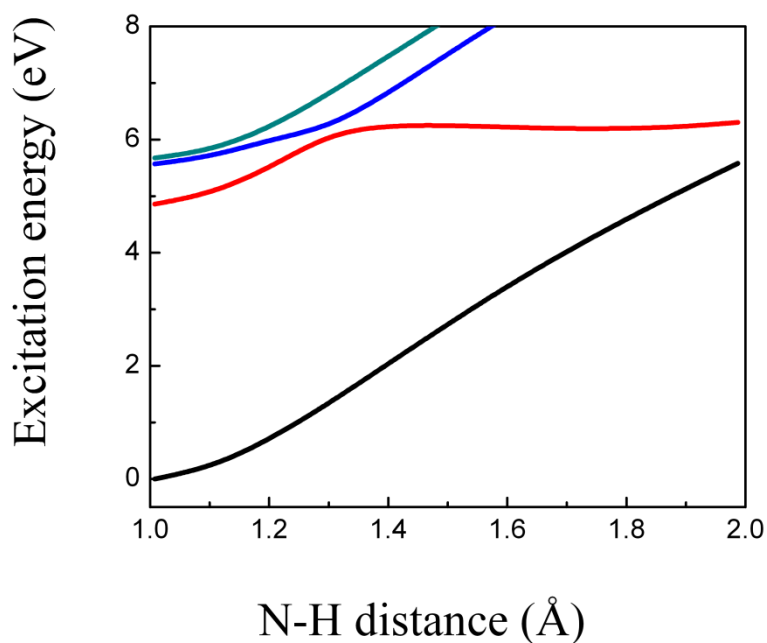
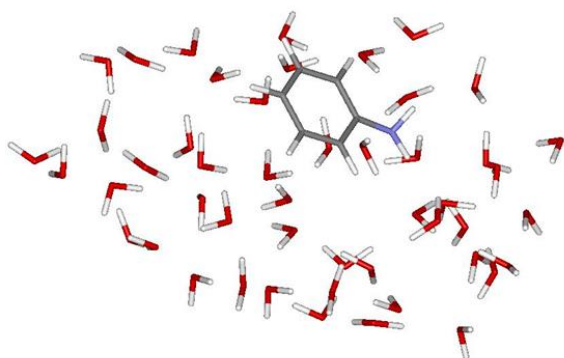


**Fig. S5:** Linear interpolation curve between the Franck-Condon region and 1<sup>1</sup> $\pi\sigma^*/S_0$  calculated for PhNH<sub>2</sub>.(H<sub>2</sub>O)<sub>2</sub>-I cluster. The ordering of the states in vFC region is given in **Table S3**.

### Aniline on the ice nanoparticles

The optimized structures of  $\text{PhNH}_2 \cdot (\text{H}_2\text{O})_{50}$  with aniline interacting via both and only one hydrogen-bonds formed between the  $\text{NH}_2$  group and oxygen atoms of clustering water molecules are presented in Figure X2. The BSSE corrected interaction energies obtained at the  $\omega\text{B97D}$  functional calculated for structures interacting via only one (Fig X2a) and both (Fig X2b) hydrogen bonds are  $-17.92$  kcal/mol and  $-22.18$  kcal/mol, respectively. Thus, structures were for both type of clustering were considered for the further calculations of the excited states.

$\text{PhNH}_2 \cdot (\text{H}_2\text{O})_{50}\text{-I}$



$\text{PhNH}_2 \cdot (\text{H}_2\text{O})_{50}\text{-II}$

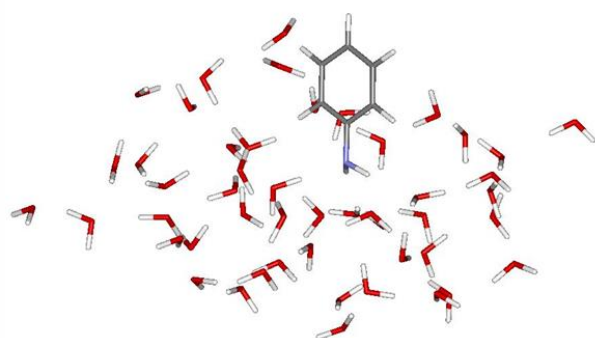


**Fig. S6:** The optimized structures of large water clusters with aniline  $\text{PhNH}_2 \cdot (\text{H}_2\text{O})_{50}$  interacting via a single or both hydrogen bonds formed between the  $\text{NH}_2$  group and oxygen atoms of the water molecules.

### References

- <sup>1</sup> G. M. Roberts, C. A. Williams, J. D. Young, S. Ullrich, M. J. Patterson and V. G. Stavros, *J. Am. Chem. Soc.*, 2012, **134**, 12578 – 12589.
- <sup>2</sup> G. A. King, T. A. A. Oliver and M. N. R. Ashfold, *J. Chem. Phys.*, 2010, **132**, 214307.

<sup>3</sup> W. E. Sinclair and D. W. Pratt, *J. Chem. Phys.*, 1996, **105**, 7942.

<sup>4</sup> T. Ebata, C. Minejima and N. Mikami, *J. Phys. Chem. A*, 2002, **106**, 11070.

<sup>5</sup> J. H. Yeh, T. L. Shen, D. G. Nocera, G. E. Leroi, I. Suzuka, H. Ozawa and Y. Namuta, *J. Phys. Chem.*, 1996, **100**, 4385 – 4389.